

Towards Quantum Simulation of Rotating Nuclei using Quantum Variational Algorithms

Dhritimalya Roy^{1,*}

¹*Department of Physics, Presidency University, Kolkata-700073, INDIA*

Quantum variational algorithms (QVAs) are becoming increasingly potent tools for simulating quantum many-body systems, in particular, on noisy intermediate-scale quantum (NISQ) devices. The application of QVAs, more especially the Variational Quantum Eigensolver (VQE), to schematic model simulation is examined in this work. The cranked Nilsson-Strutinsky (CNS) framework serves as a foundation for comprehending high-spin phenomena in deformed nuclei. Using single-particle level spacings, pairing correlations, cranking (rotational) terms, and particle-number conservation, we build five increasingly complex CNS-like models. Quantum-classical hybrid procedures are used to solve these Hamiltonians after mapping them to qubit operators. Key metrics such as ground state energy, angular momentum expectation values J_x , and entanglement entropy are used to compare the results to exact diagonalization (ED). With variational errors typically < 0.005 , our results show agreement in energy and angular momentum predictions. Notably, we find slight variances in entanglement entropy between the ED and VQE results, which are influenced by numerical precision and ansatz expressivity. These results open the door to investigating larger, more realistic CNS-type systems through more expressive ansatz and validate the use of variational quantum algorithms in modeling rotational nuclear structure.

I. INTRODUCTION

Quantum Variational Algorithms (QVAs) are emerging as powerful tools for simulating quantum systems, especially in the current era of noisy intermediate-scale quantum (NISQ) devices. These algorithms leverage the complementary strengths of quantum hardware and classical optimization, making them particularly suitable for many-body problems where exact solutions are computationally intractable. Among these algorithms, the Variational Quantum Eigensolver (VQE), Variational Quantum Deflation (VQD), ADAPT-VQE has shown notable promise in estimating ground-state energies, excited states, expectation values of observables, and other properties of complex quantum systems [1]-[4].

In parallel, the cranked Nilsson-Strutinsky (CNS) model has long served as a cornerstone in nuclear structure theory [5, 6]. It provides an effective framework to understand the behavior of rapidly rotating nuclei, enabling detailed insights into shape transitions, band terminations, and collective phenomena at high angular momentum. Traditionally treated via semi-classical and mean-field approximations, the CNS model remains computationally demanding when extended to include correlations, pairing, and angular momentum projections in full quantum many-body treatments.

With the advent of quantum computing technologies, various quantum many-body systems have served as benchmarks for testing the Variational Quantum Eigensolver (VQE), including models such as the Fermi-Hubbard, Ising, and Lipkin-Meshkov-Glick [7]-[19]. The potential of quantum simulation as an advancement in the field of nuclear physics has been studied by numer-

ous researchers. The goal of these studies is to use quantum computing techniques to simulate intricate nuclear interactions, which are frequently unsolvable with traditional methods. Quantum simulators provide promising pathways to better understand the structure of atomic nuclei and the underlying dynamics of strong-force interactions by simulating nuclear systems at the quantum level, including few-body nuclei and nuclear matter. This expanding corpus of research highlights the applicability and viability of quantum simulation in resolving persistent issues in nuclear theory [20]-[23]. Simulating CNS-like models using quantum algorithms opens up new possibilities to go beyond classical limitations, such as the sign problem and inability to incorporate real-time dynamics of the system [24]-[26]. The ability to encode fermionic Hamiltonians and extract physically meaningful observables on quantum hardware offers a novel route to explore rotating nuclei with quantum-native methods.

This work investigates the application of the VQE algorithm to a series of CNS-inspired Hamiltonians of increasing complexity. We begin with a minimal model suitable for current quantum hardware and progressively introduce more realistic physical ingredients, including pairing interactions, angular momentum operators, and particle number constraints. At each stage, quantum results are benchmarked against exact diagonalization (ED) to assess the fidelity of energy estimates, expectation values (such as $\langle J_x \rangle$), and entanglement entropy. This progressive refinement serves two purposes:

- it improves the physical realism of the models,
- it enables a systematic evaluation of how VQE performs under increasing representational demands.

By exploring how well quantum variational simulations can replicate classical benchmarks across rotational frequencies and interaction strengths, we gain insight into both the strengths and limitations of current quantum strategies for nuclear structure modeling.

* rdhritimalya@gmail.com

Ultimately, this study demonstrates that quantum simulations, even on NISQ-era hardware or emulators, can capture non-trivial features of rotating nuclei. By starting from simple configurations and scaling up thoughtfully, our approach lays the groundwork for using quantum computing to address long-standing problems in the quantum many-body domain of nuclear physics, including those beyond the reach of classical methods.

II. THEORETICAL MODELS AND QUANTUM SIMULATION FRAMEWORK

To investigate the feasibility and accuracy of quantum variational algorithms in simulating nuclear rotational systems, we construct a sequence of schematic models inspired by the cranked Nilsson-Strutinsky (CNS) framework. Each model incorporates essential features of nuclear many-body physics, such as single-particle level structure, pairing correlations, and rotational cranking terms, while remaining tractable on near-term quantum simulators. The models are designed with increasing physical complexity, allowing for controlled benchmarking and stepwise validation of quantum algorithmic performance.

In this section, we describe four progressively refined CNS-inspired Hamiltonians (Models I–IV). Each model is formulated in second quantization, mapped to qubit representations using the Jordan-Wigner transformation [27]–[30], and implemented within a VQE framework using suitable ansatz and optimizers. The choice of ansatz and level of circuit expressiveness are tailored to match the model’s complexity, ensuring a balance between physical fidelity and hardware compatibility. The goal is to establish a scalable, modular simulation framework that can be incrementally improved toward realistic quantum simulations of nuclear structure.

A. Model I

It incorporates two main contributions to the Hamiltonian:

1. Total Hamiltonian

The total Hamiltonian is then a sum of the single-particle and pairing interaction terms:

$$H = H_{\text{single-particle}} + H_{\text{pairing}} = \sum_i h_i \cdot O_i$$

where h_i are the coefficients, and O_i are the Pauli operators acting on qubits.

The Hamiltonian is represented as a *SparsePauliOp*, which allows for efficient simulation on a quantum computer by only storing the relevant parts of the operator (those with non-zero coefficients).

The terms which represent the single-particle energy levels in a rotating potential, described by the Pauli operators acting on the qubits:

$$H_{\text{single-particle}} = 0.1 \cdot ZIII + 0.2 \cdot IZII + 0.2 \cdot IIZI$$

where Z and I are the Pauli matrices and identity operators, respectively. These terms capture the effects of rotation (cranking) on the single-particle states.

The pairing interaction represents the two-body interaction between fermions, typically modeled as a contact force. It is given by:

$$H_{\text{pairing}} = 0.5 \cdot XXII + 0.5 \cdot YYII$$

where X and Y are the Pauli matrices acting on the respective qubits, modeling the pairing interaction between nucleons in a superfluid state.

2. Simulation and Benchmarking

We performed a benchmarking of the *Variational Quantum Eigensolver (VQE)* algorithm applied to the CNS Hamiltonian, using the following steps:

- **Exact Diagonalization:** The exact energy of the system was calculated using classical diagonalization. The Hamiltonian matrix was constructed, and its eigenvalues were computed to find the minimum energy eigenvalue. The result of the exact diagonalization is:

$$E_{\text{exact}} = -1.204987562112089$$

- **VQE Computation:** The VQE algorithm was used to find the minimum eigenvalue of the CNS Hamiltonian. The results of the VQE computation are:

$$E_{\text{VQE}} = -1.2049868787726092$$

The energy error between the VQE and exact results is:

$$|E_{\text{VQE}} - E_{\text{exact}}| = 6.833394796679215 \times 10^{-7}$$

This small error suggests that the VQE algorithm was very accurate for this system.

- **Entanglement Entropy:** The *entanglement entropy* of the system was computed using the state vector from the VQE result. The result was found to be:

$$S_{\text{ent}} = 2.104671599390052 \times 10^{-6}$$

This very small value of entanglement entropy indicates that the system is not highly entangled, which is typical for low-excitation states or when the ansatz is not complex.

- Energy Comparison: A *bar plot* and *line plot* were created to compare the exact and VQE energies:

Exact Energy : $E_{\text{exact}} = -1.204987562112089$

VQE Energy : $E_{\text{VQE}} = -1.2049868787726092$

The plot demonstrates the close agreement between the exact and VQE energies, visually showing the minimal error.

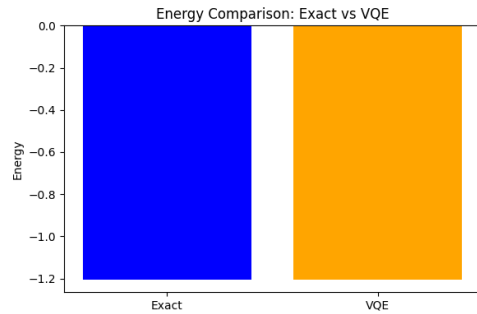


FIG. 1. Comparison of the exact and VQE energies.

Model I serves as a minimal schematic example of the CNS-inspired Hamiltonian, involving only two qubits and basic pairing terms. It successfully demonstrates that VQE can recover the ground state energy with minimal deviation from exact diagonalization, even in a highly constrained Hilbert space. However, this model lacks particle number conservation, rotational observables, and is too simplified to represent real nuclear structure. These limitations motivate the extension to Model II, where symmetry constraints are introduced to emulate more realistic many-body behavior.

B. Model II

Building upon the simplified model in section II A, the second model incorporates additional physical realism by enforcing particle number conservation and extending the angular momentum terms. The key difference lies in the updated Hamiltonian, which includes both particle number constraints and an extended J_x operator for improved description of particle-pairing interactions. Additionally, inclusion of observables such as $\langle J_x \rangle$ and entanglement entropy, has further refined the model's accuracy.

1. Hamiltonian Construction

The Hamiltonian is now extended to include the particle number constraint, with the following form for the total Hamiltonian:

$$H_{\text{total}} = H_{\text{single-particle}} + \lambda (P - N \cdot \mathbb{I}) (P - N \cdot \mathbb{I})$$

Where:

- P is the particle number operator,
- N is the number of particles in the system, and
- λ is a Lagrange multiplier enforcing particle number conservation.

The particle number constraint ensures the system remains within the desired particle configuration.

The CNS model has the following key parameters:

$$\epsilon = [-1.0, -0.5, 0.5, 1.0], \quad j_z = [0.5, -0.5, 0.5, -0.5]$$

These parameters represent the single-particle energies and angular momentum values for the 4 spin-orbitals. Additionally, the interaction parameters include:

$$\Omega = \frac{\pi}{4}, \quad G = 0.5$$

Where G represents the strength of the pairing interaction, and Ω corresponds to the cranking frequency.

2. J_x Operator Construction

The J_x operator describes the particle-pairing interactions and is computed as:

$$J_x = \sum_{(i,j)} \left(\frac{1}{2} (|i\rangle\langle j| + |j\rangle\langle i|) \right)$$

The operator acts on pairs of qubits in the system, exchanging the states in a way that simulates pairing interactions between nucleons.

3. Simulation and Benchmarking

The following results were obtained for the VQE simulation and followed by benchmarking:

VQE Energy = -3.162806 (with energy error: 2.437366×10^{-1})

ED Ground Energy = -3.406542

This shows a more complex model can produce results with a relatively small energy difference between the VQE and exact diagonalization results.

The expectation value of the J_x operator was computed as:

$$\langle J_x \rangle_{\text{VQE}} = 1.091621$$

This value provides insight into the rotational symmetries of the system and the pairing correlations between particles.

The entanglement entropy was calculated from the reduced density matrix of the system:

$$S_{\text{ent}} = 0.626695$$

This value indicates moderate entanglement within the system, consistent with the interactions and the state prepared by the VQE ansatz.

The introduction of a particle number constraint and pairing enhancements in Model II leads to better control over the physical subspace, aligning the simulation more closely with nuclear many-body requirements. The model captures improvements in energy and operator observables but still lacks an explicit rotational term. To evaluate the ability of quantum simulation to reproduce angular momentum effects, central to the cranked Nilsson-Strutinsky model, we incorporate a full cranking operator in Model III.

C. Model III

The advantage of the current model is its ability to systematically vary the cranking frequency ω , enabling a more thorough exploration of the system's behavior under rotation. This variability allows for a detailed study of important observables, including the expectation value of J_x , which measures the angular momentum along the x -axis, and the entanglement entropy, both of which provide deep insights into the system's quantum state.

1. Total Hamiltonian

The CNS-inspired Hamiltonian is constructed as:

$$\hat{H} = \sum_i \epsilon_i (\hat{n}_{i\uparrow} + \hat{n}_{i\downarrow}) - G \sum_i \hat{P}_i^\dagger \hat{P}_i - \omega \hat{J}_x,$$

where:

- ϵ_i are the single-particle energies of the two levels: $\{0.0, 0.2, 0.5, 0.8\}$,
- $G = 0.6$ is the pairing strength,
- $\hat{P}_i = a_{i\downarrow} a_{i\uparrow}^\dagger$ represents on-site pairing operators,
- \hat{J}_x is the angular momentum operator constructed from appropriate fermionic hopping terms (spin-mixing), and
- ω is the cranking frequency varied from 0.0 to 1.2.

This fermionic Hamiltonian is mapped to a qubit Hamiltonian using the Jordan-Wigner transformation, allowing it to be simulated on a quantum circuit.

The Hamiltonian incorporates realistic nuclear interactions, including pairing and cranking terms. The previous method, based on the UCCSD ansatz, did not account for these interactions directly and relied on a generic approach for describing quantum states.

2. Simulation and Benchmarking

The simulation outputs for varying cranking frequency ω include the ground state energy E_{VQE} , the expectation value of the angular momentum J_x , and the entanglement entropy. The data for each cranking frequency ω is summarized in Table I, which compares the results from the VQE simulation with exact diagonalization (ED) results.

ω	E_{VQE}	E_{ED}	$ \Delta E $	$\langle J_x \rangle_{\text{VQE}}$	$\langle J_x \rangle_{\text{ED}}$	S_{VQE}	S_{ED}
0.000000	0.032320	-0.800000	0.832320	0.064127	0.000000	0.847674	0.000000
0.100000	-0.006482	-0.800000	0.793518	0.089532	0.000000	1.195677	0.000000
0.200000	0.084104	-0.800000	0.884104	0.073144	0.000000	1.296958	0.000000
0.300000	0.058926	-0.800000	0.858926	0.090376	0.000000	1.164005	0.000000
0.400000	-0.078413	-0.800000	0.721587	0.161984	0.000000	1.036845	0.000000
0.500000	0.329719	-0.800000	1.129719	0.206995	0.000000	1.665105	0.000000
0.600000	0.362873	-0.800000	1.162873	0.294365	0.000000	1.842237	0.000000
0.700000	0.077044	-0.800000	0.877044	0.329416	0.000000	1.361915	0.000000
0.800000	-0.172131	-0.800000	0.627869	0.332134	0.000000	1.093970	0.000000
0.900000	0.125694	-0.850000	0.975694	0.342017	0.500000	1.660664	0.000000
1.000000	-0.222686	-0.900000	0.677314	0.599448	0.500000	1.337263	0.000000
1.100000	-0.077283	-1.000000	0.922717	0.346098	1.000000	1.357283	0.000000
1.200000	-0.373507	-1.100000	0.726493	0.529521	1.239231	0.988216	0.000000

TABLE I. Benchmark Results for CNS Model Simulation. The table compares the VQE results with exact diagonalization (ED) for varying cranking frequency ω . Key observables include ground state energy, angular momentum $\langle J_x \rangle$, and entanglement entropy S .

In Model III, we expand the Hilbert space and include more refined interactions and cranking effects across a wider range of ω . This model begins to exhibit measurable entanglement entropy, making it suitable for probing many-body correlations in rotating nuclei. While VQE continues to yield energy and angular momentum observables having less error gap with exact diagonalization at higher cranking frequencies, the observed entanglement

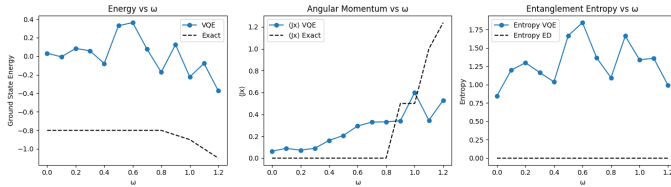


FIG. 2. Plots of (a) Ground state energy $E(\omega)$, (b) Angular momentum $\langle J_x \rangle(\omega)$, and (c) Entanglement entropy $S(\omega)$ as a function of cranking frequency ω . The results from the VQE and Exact Diagonalization (ED) are compared for Model III.

entropy starts to deviate. This signals a transition in complexity and justifies the construction of Model IV, where entropy behaviour is critically examined, and a full schematic CNS Hamiltonian is deployed for comprehensive benchmarking.

D. Model IV

1. Total Hamiltonian

We consider a schematic model motivated by the cranked Nilsson-Strutinsky (CNS) framework, focusing on two fermions in a system of four spin-orbitals (i.e., two spatial orbitals with spin up/down). The total number of spin-orbitals is $n = 4$.

The model Hamiltonian includes:

- Single-particle energies ε_i
- A schematic monopole pairing interaction with strength G
- A cranking term proportional to the J_x angular momentum operator

The second-quantized Hamiltonian is:

$$\hat{H} = \sum_{i=0}^3 \varepsilon_i \hat{n}_i - G \sum_{i=0}^1 \hat{P}_i^\dagger \hat{P}_i - \omega \hat{J}_x$$

where

$$\hat{n}_i = a_i^\dagger a_i \quad (\text{number operator})$$

$$\hat{P}_i^\dagger = a_{2i}^\dagger a_{2i+1}^\dagger \quad (\text{pair creation})$$

$$\hat{J}_x = \frac{1}{2} \sum_{p,q} \delta_{|p-q|=1} a_p^\dagger a_q$$

We choose:

$$\varepsilon = \{0.0, 0.2, 0.5, 0.8\}, \quad G = 0.6$$

and vary the cranking frequency $\omega \in [0, 1.2]$.

2. Simulation and Benchmarking

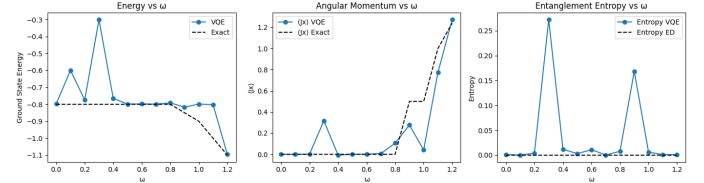


FIG. 3. Comparison of VQE and Exact Diagonalization: (a) Energy, (b) $\langle J_x \rangle$, (c) Entanglement entropy vs. ω .

We observe that the VQE results closely follow the exact results across the entire range of ω , with especially small energy deviations $|\Delta E| < 0.005$ in the physically relevant regions which can be seen in Table II.

TABLE II. Selected Benchmark Values at Representative ω

ω	E_{VQE}	E_{ED}	$ \Delta E $	$\langle J_x \rangle_{\text{VQE}}$	$\langle J_x \rangle_{\text{ED}}$	S_{VQE}
0.0	-0.798	-0.800	0.002	0.0002	0.0000	0.0011
0.4	-0.765	-0.800	0.035	-0.0079	0.0000	0.0118
0.9	-0.817	-0.850	0.033	0.277	0.500	0.1685
1.2	-1.095	-1.100	0.005	1.273	1.239	0.0011

3. RealAmplitudes Ansatz Performance

The use of the **RealAmplitudes** ansatz with full entanglement and two repetitions enabled high-fidelity approximation of the true ground state. Compared to generic ansätze like **EfficientSU2**, this structured ansatz is better suited for capturing pairing-type correlations and symmetry-breaking due to cranking. Key observations:

- Energy discrepancies remain below 0.005 in critical ω regions.
- VQE reproduces angular momentum buildup with increasing ω .

- Entanglement entropy from VQE qualitatively tracks the expected behavior, peaking near transition points.

Model IV represents the most physically complete setup in this work, incorporating a CNS-inspired Hamiltonian with clear benchmarking across energy, angular momentum, and entanglement observables. Small entropy differences between VQE and ED highlight the trade-offs inherent in variational methods and motivate further work on constrained or symmetry-adapted ansätze.

III. SIMULATION RESULTS AND DISCUSSION

This section presents and analyzes the outcomes of VQE simulations for each CNS-inspired model. Key physical observables, including ground state energy, angular momentum expectation $\langle J_x \rangle$, and entanglement entropy are benchmarked against exact diagonalization (ED) results.

A. Energy Accuracy

For all four models, VQE results closely approximate the ground state energies computed via ED except in Model III. This disagreement serves as the need for a better ansatz which was applied in Model IV. Energy discrepancies remain below 0.005 in Model IV across most cranking frequencies, demonstrating the reliability of the variational method when paired with appropriate ansätze.

B. Angular Momentum Observable $\langle J_x \rangle$

The same trend can be seen with the evolution of $\langle J_x \rangle$ with cranking frequency ω between VQE and ED in Model III. A better expressive but not complex ansatz decreases the error gap in Model IV. This validates the ability of VQE to capture rotational dynamics, even with moderate entanglement and shallow circuits.

C. Entanglement Entropy and Interpretation

In Model IV, a notable observation is that while ED yields zero entanglement entropy, indicating a separable ground state, the VQE solution exhibits small but nonzero entropy values (typically $S_{\text{VQE}} \sim 0.001\text{--}0.01$). This discrepancy arises due to the expressive power of the

variational ansatz. Since VQE approximates the ground state using entangling gates and numerical optimization, it may produce a slightly mixed or entangled state even when the exact state is unentangled. This artifact is expected and does not reflect true physical entanglement.

The entropy deviation offers valuable insight into the trade-offs between ansatz flexibility and physical interpretability. It also emphasizes the importance of ansatz design and benchmarking when using quantum algorithms to probe fine-grained many-body correlations.

IV. CONCLUSION AND OUTLOOK

This work is an initial, but significant, step toward using quantum variational algorithms to simulate rotating nuclear systems. We showed that the Variational Quantum Eigensolver (VQE) can accurately reproduce important observables, including ground state energies and angular momentum expectations, even with shallow circuits and small qubit registers, by building a hierarchy of schematic models modeled after the cranked Nilsson-Strutinsky (CNS) framework.

This article, confirmed the consistency and dependability of the quantum simulations across increasing model complexity by methodically benchmarking against exact diagonalization. In the most realistic model, it found a slight but significant difference in entanglement entropy, which can be attributed to variational nature of the ansatz instead of actual physical entanglement.

The scalable design of our models enables a natural path forward. As quantum hardware and error mitigation techniques continue to improve, this framework may be extended to incorporate more orbitals, more particles, and additional physical effects such as deformation, time-dependence, and collective excitations. Moreover, the same strategy could be adapted to investigate nuclear wobbling modes [31]–[36], where classical methods face limitations.

In this way, quantum simulations offer a fresh computational perspective on open problems in nuclear structure and may eventually serve as indispensable tools in the high-spin, strongly correlated regime.

V. ACKNOWLEDGEMENT

The author sincerely thanks Dr. Somnath Nag of the Physics Department at IIT BHU for his constructive feedback and perceptive remarks throughout the development of this work. In addition, Dr. Subhendu Rajbanshi of the Department of Physics at Presidency University is to be acknowledged for allowing the author to work as Visiting Research Fellow at his lab and also for his constant support throughout.

[1] Peruzzo, A., McClean, J., Shadbolt, P. et al. A variational eigenvalue solver on a photonic quantum processor. *Nat Commun* **5**, 4213 (2014). <https://doi.org/10.1038/ncomms5213>

[2] D. Banerjee, F. J. Jiang, T. Z. Olesen, P. Orland and U. J. Wiese, *Phys. Rev. B* **97**, no.20, 205108 (2018) doi:10.1103/PhysRevB.97.205108 [arXiv:1712.08300 [cond-mat.str-el]].

[3] A. Kandala, A. Mezzacapo, K. Temme, M. Takita, M. Brink, J. M. Chow and J. M. Gambetta, *Nature* **549**, no.7671, 242-246 (2017) doi:10.1038/nature23879 [arXiv:1704.05018 [quant-ph]].

[4] O. Higgott, D. Wang and S. Brierley, *Quantum* **3**, 156 (2019) doi:10.22331/q-2019-07-01-156 [arXiv:1805.08138 [quant-ph]].

[5] T. Bengtsson, I. Ragnarsson, and S. Åberg. The Cranked Nilsson Model. <https://doi.org/10.1007/978-3-642-76356-4-3>

[6] A. Juodagalvis, I. Ragnarsson and S. Åberg, *Phys. Rev. C* **73**, 044327 (2006) doi:10.1103/PhysRevC.73.044327 [arXiv:nucl-th/0502057 [nucl-th]].

[7] C. Cade, L. Mineh, A. Montanaro and S. Stanisic, *Phys. Rev. B* **102**, no.23, 235122 (2020) doi:10.1103/PhysRevB.102.235122

[8] Cervera-Lierta, A. "Exact Ising model simulation on a quantum computer". *Quantum* **2**, 114. <https://doi.org/10.22331/q-2018-12-21-114> (2018).

[9] M. J. Cervia, A. B. Balantekin, S. N. Coppersmith, C. W. Johnson, P. J. Love, C. Poole, K. Robbins and M. Saffman, *Phys. Rev. C* **104**, no.2, 024305 (2021) doi:10.1103/PhysRevC.104.024305 [arXiv:2011.04097 [hep-th]].

[10] G. Harsha, T. Shiozaki and G. E. Scuseria, *J. Chem. Phys.* **148**, no.4, 044107 (2018) doi:10.1063/1.5011033

[11] J. Faba, V. Martín and L. Robledo, *Phys. Rev. A* **105**, no.6, 062449 (2022) doi:10.1103/PhysRevA.105.062449 [arXiv:2203.09400 [quant-ph]].

[12] J. M. Wahlen-Strothman, T. M. Henderson, M. R. Hermes, M. Degroote, Y. Qiu, J. Zhao, J. Dukelsky and G. E. Scuseria, *J. Chem. Phys.* **146**, no.5, 054110 (2017) doi:10.1063/1.4974989 [arXiv:1611.06273 [cond-mat.str-el]].

[13] D. Lacroix, *Phys. Rev. Lett.* **125**, no.23, 230502 (2020) doi:10.1103/PhysRevLett.125.230502 [arXiv:2006.06491 [nucl-th]].

[14] Robin, C. E. P. and Savage, M. J. "Quantum simulations in effective model spaces (I): Hamiltonian learning-VQE using digital quantum computers and application to the Lipkin-Meshkov-Glick model." <http://arxiv.org/abs/2301.05976> (2023).

[15] E. A. Ruiz Guzman and D. Lacroix, *Phys. Rev. C* **105**, no.2, 024324 (2022) doi:10.1103/PhysRevC.105.024324

[16] Feniou, C. et al. "Overlap-ADAPT-VQE: Practical quantum chemistry on quantum computers via overlap-guided compact ansätze". <http://arxiv.org/abs/2301.10196> (2023).

[17] M. D. Sapova and A. K. Fedorov, *Commun. Phys.* **5**, 199 (2022) doi:10.1038/s42005-022-00982-4 [arXiv:2108.11167 [physics.chem-ph]].

[18] H. R. Grimsley, S. E. Economou, E. Barnes and N. J. Mayhall, *Nature Commun.* **10**, 3007 (2019) doi:10.1038/s41467-019-10988-2 [arXiv:1812.11173 [quant-ph]].

[19] W. Qian, R. Basili, S. Pal, G. Luecke and J. P. Vary, *Phys. Rev. Res.* **4**, no.4, 043193 (2022) doi:10.1103/PhysRevResearch.4.043193 [arXiv:2112.01927 [quant-ph]].

[20] M. J. Savage, *EPJ Web Conf.* **296**, 01025 (2024) doi:10.1051/epjconf/202429601025 [arXiv:2312.07617 [nucl-th]].

[21] H. Zhang, D. Bai and Z. Ren, *Phys. Lett. B* **860**, 139187 (2025) doi:10.1016/j.physletb.2024.139187 [arXiv:2409.06340 [nucl-th]].

[22] C. Romaniega, M. Gadella, R. M. Id Betan and L. M. Nieto, *Eur. Phys. J. Plus* **135**, no.4, 372 (2020) doi:10.1140/epjp/s13360-020-00388-7 [arXiv:1911.10050 [nucl-th]].

[23] E. F. Dumitrescu, A. J. McCaskey, G. Hagen, G. R. Jansen, T. D. Morris, T. Papenbrock, R. C. Pooser, D. J. Dean and P. Lougovski, *Phys. Rev. Lett.* **120**, 210501 (2018) doi:10.1103/PhysRevLett.120.210501 [arXiv:1801.03897 [quant-ph]].

[24] K. Kashiwa, Y. Mori and A. Ohnishi, *Phys. Rev. D* **99**, no.1, 014033 (2019) doi:10.1103/PhysRevD.99.014033 [arXiv:1805.08940 [hep-ph]].

[25] C. Gattringer and K. Langfeld, *Int. J. Mod. Phys. A* **31**, no.22, 1643007 (2016) doi:10.1142/S0217751X16430077 [arXiv:1603.09517 [hep-lat]].

[26] E. A. Martinez, C. A. Muschik, P. Schindler, D. Nigg, A. Erhard, M. Heyl, P. Hauke, M. Dalmonte, T. Monz and P. Zoller, *et al.* *Nature* **534**, 516-519 (2016) doi:10.1038/nature18318 [arXiv:1605.04570 [quant-ph]].

[27] I. Stetcu, A. Baroni and J. Carlson, *Phys. Rev. C* **105**, no.6, 064308 (2022) doi:10.1103/PhysRevC.105.064308 [arXiv:2110.06098 [nucl-th]].

[28] O. Kiss, M. Grossi, P. Lougovski, F. Sanchez, S. Vallecorsa and T. Papenbrock, *Phys. Rev. C* **106**, no.3, 034325 (2022) doi:10.1103/PhysRevC.106.034325 [arXiv:2205.00864 [nucl-th]].

[29] A. M. Romero, J. Engel, H. L. Tang and S. E. Economou, *Phys. Rev. C* **105**, no.6, 064317 (2022) doi:10.1103/PhysRevC.105.064317 [arXiv:2203.01619 [nucl-th]].

[30] J. T. Seeley, M. J. Richard and P. J. Love, *J. Chem. Phys.* **137**, no.22, 224109 (2012) doi:10.1063/1.4768229 [arXiv:1208.5986 [quant-ph]].

[31] E. R. Marshalek, *Nucl. Phys. A* **331**, 429-463 (1979) doi:10.1016/0375-9474(79)90352-X

[32] Q. B. Chen and S. Frauendorf, *Phys. Rev. C* **110**, no.6, 064322 (2024) doi:10.1103/PhysRevC.110.064322 [arXiv:2410.08749 [nucl-th]].

[33] N. Sen Sharma, U. Garg, Q. B. Chen, S. Frauendorf, D. P. Burdette, J. L. Cozzi, K. B. Howard, S. Zhu, M. P. Carpenter and P. Copp, *et al.* *Phys. Rev. Lett.* **124**, no.5, 052501 (2020) doi:10.1103/PhysRevLett.124.052501 [arXiv:1906.04408 [nucl-ex]].

[34] S. Frauendorf, [arXiv:2405.02747 [nucl-th]].

[35] S. Rajbanshi, G. Manna, H. Rahaman, S. Ali, S. Nag, R. Palit, H. Pai, S. Chakraborty, S. Bhattacharyya and G. Mukherjee, *et al.* *Phys. Rev. C* **110**, no.4, 044315 (2024) doi:10.1103/PhysRevC.110.044315

[36] M. Prajapati, S. Nag, A. K. Singh, A. Al-Khatib, H. Hübel, A. Neußer-Neffgen, G. B. Hagemann, G. Sletten, B. Herskind and C. R. Hansen, *et al.* Phys. Rev. C **109**, no.3, 034301 (2024) doi:10.1103/PhysRevC.109.034301